Particle distributions in electroweak tachyonic preheating[*]

Jon-Ivar Skullerud, Jan Smit and Anders Tranberg[a]

[a]ITF, University of Amsterdam, Valckenierstraat 65, 1018 XE Amsterdam, The Netherlands

We consider the out-of-equilibrium (quasi-) particle number distributions of the Higgs and W-fields during electroweak tachyonic preheating. We model this process by a fast quench, and perform classical real-time lattice simulations in the SU(2)–Higgs model in three dimensions. We discuss how to define particle numbers and effective energies using two-point functions in Coulomb and unitary gauge, and consider some of the associated problems. After an initial exponential growth in effective particle numbers, the system stabilises, allowing us to extract effective masses, temperatures and chemical potentials for the particles.

1. INTRODUCTION

In recent scenarios of electroweak baryogenesis [1,2] the electroweak transition is assumed to have taken place at low (zero) temperature shortly after inflation, by the effective mass-squared parameter of the Higgs field changing sign from positive to negative ('tachyonic'). An important issue in this scenario is the time needed for the system to reach approximate thermalisation, and the resulting effective temperature. The temperature must be low enough and the thermalisation sufficiently rapid that sphaleron transitions that can wash out the generated baryon asymmetry are prevented. One of the main aims of this study is to determine the effective temperature.

We employ the classical approximation, which allows us to study fields far from equilibrium non-perturbatively by numerical simulation. In our case, this approximation should be justified [3] since the instability resulting from the change of sign in the mass-squared parameter leads to exponentially growing, and hence large, occupation numbers. The full results are presented in [4].

2. PARTICLE DISTRIBUTIONS

The definition of particle numbers and energies in an interacting field theory out of equilibrium is not unique. Furthermore, in a non-abelian gauge theory the two-point correlators used to define them may be gauge dependent. Here, the natural

choice of gauge for the Higgs doublet ϕ is the unitary gauge, where it only has one non-zero real component $\phi = (0, h/\sqrt{2})^T$. For the gauge fields, we will study the particle distribution in both the unitary gauge and the Coulomb gauge $\partial_i A_i = 0$.

We use a method [5,6] where effective particle numbers and energies are determined selfconsistently, in analogy with the free-field quantum correlators. For the Higgs field (with $\pi_h = \dot{h}$), they are defined as

$$n_k^H \equiv \sqrt{\langle h(\vec{k})h(-\vec{k})\rangle_C \langle \pi_h(\vec{k})\pi_h(-\vec{k})\rangle_C}\,, \qquad (1)$$

$$\omega_k^H \equiv \sqrt{\frac{\langle \pi_h(\vec{k})\pi_h(-\vec{k})\rangle_C}{\langle h(\vec{k})h(-\vec{k})\rangle_C}}\,, \qquad (2)$$

where $\langle \cdots \rangle_C$ is the connected two-point function given by $\langle AB \rangle_C \equiv \langle AB \rangle - \langle A \rangle \langle B \rangle$, and we have suppressed the common time coordinate t.

The gauge field correlators $\langle A_i^a(k)A_j^b(-k)\rangle = \delta^{ab}C_{ij}^{AA}(\vec{k})$ can be decomposed in a transverse and a longitudinal part, as

$$C_{ij}^{AA}(\vec{k}) = \left(\delta_{ij} - \frac{k_i k_j}{k^2}\right)D_T^A(k) + \frac{k_i k_j}{k^2}D_L^A(k)\,, \quad (3)$$

and analogously for the canonical momentum field $E_i^a = F_{i0}^a$. In the Coulomb gauge the gauge potential is purely transverse, and n_k^A and ω_k^A can be defined as

$$n_k^A \equiv \sqrt{D_T^A(k)D_T^E(k)}\,, \qquad \omega_k^A \equiv \sqrt{\frac{D_T^E(k)}{D_T^A(k)}}\,. \quad (4)$$

In the unitary gauge, the transverse n_k^T and ω_k^T are found to be the same as for the Coulomb
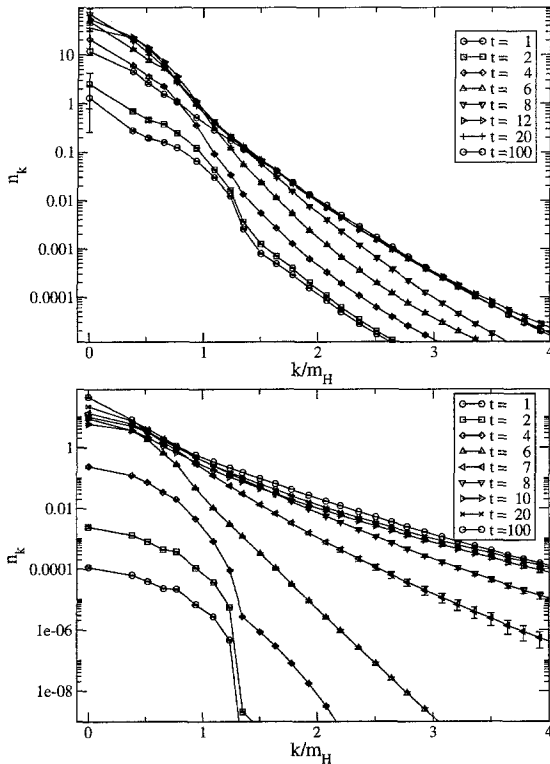
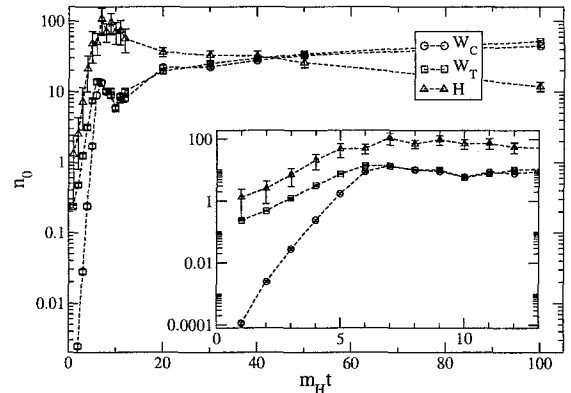Figure 1. Higgs (top) and Coulomb-gauge W (bottom) particle distributions for different times.

Figure 2. Particle numbers of the zero-modes as a function of time. H: Higgs; W_T: transverse W in unitary gauge; W_C: transverse W in Coulomb gauge.

gauge, while the longitudinal occupation numbers and mode energies, assuming the form $\omega_k^{L2} = m_{\text{eff}}^2 + k^2$, are given by [4]

$$n_k^L = \sqrt{D_L^A(k)D_L^E(k)}, \quad \omega_k^L = m_{\text{eff}}^2 \sqrt{\frac{D_L^A(k)}{D_L^E(k)}}. \quad (5)$$

3. RESULTS

We have performed simulations on a volume $L^3 = 21^3 m_H^{-3}$ with $g = 2/3, \lambda = 1/9$, giving $m_H^2/m_W^2 = 2$, with lattice spacing $a = 0.35\,m_H^{-1}$. We initialise the system according to the "Just the half" scheme introduced and explained in [3]. The Higgs field is initialised by generating classical realisations of an ensemble reproducing the quantum vacuum correlators. We assume that the Higgs field is in the symmetric phase ($\langle\phi\rangle = 0$) with an effective mass parameter $\mu_{\text{eff}}^2 = \mu^2 > 0$,

and approximately free field fluctuations

$$\langle\phi(k)\phi(k)^\dagger\rangle = \frac{1}{2\omega(k)}, \quad \langle\pi(k)\pi(k)^\dagger\rangle = \frac{\omega(k)}{2}, \quad (6)$$

with $\omega(k) = \sqrt{\mu^2 + k^2}$. However, we only initialise the unstable ($|k| < |\mu|$) modes. The gauge potential A is initialised to zero, while the E-field is constructed to satisfy the Gauss constraint.

We model the transition where μ_{eff}^2 goes through zero as a quench, in which μ_{eff}^2 flips its sign from μ^2 to $-\mu^2$ instantaneously. 42 independent realisations of the initial conditions (6) have been generated, and the subsequent time evolution sampled for $tm_H = 1, 2, \ldots, 12, 20, 30, 40, 50, 100$. Nearby momenta have been averaged within 'bins' of size $\Delta = 0.05a^{-1} = 0.0175m_H$

Figure 1 shows the particle distributions for the Higgs and Coulomb-gauge W fields. In both cases we see the occupation numbers of the low-momentum modes increasing exponentially up to $t \approx 6 - 8\,m_H^{-1}$. At this point the low-momentum modes start saturating, while the high-momentum modes rapidly become populated. After $t \approx 20\,m_H^{-1}$ the system evolves only very slowly, with an approximately exponential distribution at late times. A similar behaviour is seen for the W fields in the unitary gauge. The W distributions in unitary and Coulomb gauge start out very different (the unitary-gauge distribution

initially being close to the Higgs distribution) but become indistinguishable after $t \approx 40\,m_H^{-1}$. The early exponential growth and subsequent slow evolution is illustrated in fig. 2, which shows the time evolution of the zero-mode occupation numbers. The exponential fall-off with momentum means that we do not expect problems with lattice artefacts due to cutoff effects.

Turning to the dispersion relation, we find qualitatively the same behaviour for the Higgs particles and the transverse W-modes in the Coulomb and unitary gauges. For $t \lesssim 20\,m_H^{-1}$ there is no sensible dispersion relation, while for $t \gtrsim 30\,m_H^{-1}$ it approaches the form $\omega^2 = m_{\rm eff}^2 + ck^2$, with $c \approx 1$ for the Higgs and Coulomb-gauge W particles. In the unitary gauge, the particle-like behaviour is slower to emerge, and the slope remains smaller than 1 (and increasing) at the latest times. For the longitudinal modes, with the 'inverse' definition (5) of the mode energy, the dispersion relation approaches a straight line only very slowly, and we do not attempt to perform a fit to the data. We fit the effective energies to the form $\omega_k^2 = ck^2 + m_{\rm eff}^2$. For the W fields, we find that the intercepts in the two gauges are compatible and change very little from $t = 40\ m_H^{-1}$ onwards, yielding a value $m_{\rm eff} \approx 0.68 m_H$, close to the zero-temperature value $0.71\,m_H$. For the Higgs fields, we find an effective mass which is somewhat smaller than the zero-temperature mass, although it appears to be increasing with time.

Taking the effective energy from the fitted dispersion relation, we then fit the particle numbers to a Bose-Einstein distribution, $n_k = [\exp((\omega_k - \mu)/T) - 1]^{-1}$. We only fit to the lowest 5 non-zero modes, for which $n_k > 0.5$ and thus the classical approximation may be expected to be valid. The best fits at the latest time $(t = 100\,m_H^{-1})$ are shown in fig. 3. We find that the effective temperature T of the Coulomb-gauge W fields stabilises from $t \approx 40\,m_H^{-1}$ onwards at $T_W \approx 0.42\,m_H$. In the unitary gauge, the temperature is lower (but increasing) due to the smaller slope in the dispersion relation. The effective Higgs temperature starts out higher but drops to $T_H \approx 0.4\,m_H$ at $t = 100\,m_H^{-1}$. In all cases, however, a large chemical potential — slightly larger even than the effective mass — is required to describe the distri-
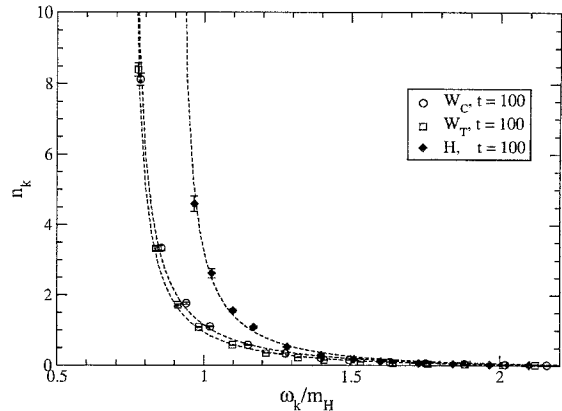

Figure 3. Higgs and W-particle numbers at $t = 100\,m_H^{-1}$ as a function of the effective energy ω taken from the fitted dispersion relation. Also shown are the best fits to the Bose–Einstein distribution. The zero-modes are outside the boundaries of the plot.

bution. This would lead to an unphysical pole in the distribution; however, the occupation numbers of the zero-modes (which are not included in the fits) lie considerably below the fits, indicating a flattening of the distribution relative to a BE form at the lowest available energies.

Acknowledgments

REFERENCES

1. J. García-Bellido, D. Y. Grigoriev, A. Kusenko and M. E. Shaposhnikov, Phys. Rev. **D60**, 123504 (1999), [hep-ph/9902449].
2. L. M. Krauss and M. Trodden, Phys. Rev. Lett. **83**, 1502 (1999), [hep-ph/9902420].
3. J. Smit and A. Tranberg, JHEP **12**, 020 (2002), [hep-ph/0211243].
4. J.-I. Skullerud, J. Smit and A. Tranberg, JHEP **08**, 045 (2003), [hep-ph/0307094].
5. G. Aarts and J. Smit, Phys. Rev. **D61**, 025002 (2000), [hep-ph/9906538].
6. M. Sallé, J. Smit and J. C. Vink, Phys. Rev. **D64**, 025016 (2001), [hep-ph/0012346].